ELSEVIER

Solid State Ionics 93 (1997) 65–84

SOLID STATE IONICS

Modelling of ambipolar transport properties of composite mixed ionic–electronic conductors

Zhonglin Wu, Meilin Liu*

School of Materials Science and Engineering, Georgia Institute of Technology, Atlanta, GA 30332-0245, USA

Received 22 April 1996; accepted 31 July 1996

Abstract

The ability to transport both ionic and electronic species is one of the most important properties of a mixed ionic–electronic conductor for electrosynthesis, gas separation, and electrode applications. In this paper, resistor network approach is used to predict the effective conductivities of a composite mixed conductor consisting of any number of randomly-distributed phases. The model is further used to predict the effective ionic, electronic, and ambipolar transport behavior of two-phase and three-phase composite mixed conductors as a function of the volume fraction of each randomly-distributed constituent phase. Results indicate that the optimum ambipolar conductivity occurs only within certain volume fractions of the constituent phases, depending on their relative ionic and electronic conductivities.

Keywords: Mixed ionic–electronic conductor; Multi-phase composite; Transport; Effective conductivity; Resistor network

1. Introduction

In recent years, mixed ionic–electronic conductors (MIECs) based on composites have found wide applications in solid-state ionic devices such as batteries, fuel cells, and chemical sensors, and in electrochemical processes such as electrosynthesis and gas separation [1–4]. The greatest advantage of a composite MIEC over a homogeneous, single phase MIEC is that the transport properties of a composite can be readily tailored for a particular application. For membrane applications, a desired composite MIEC consists of two continuously distributed phases, one being predominantly ionically conductive and the other being predominantly electronically conductive. Accordingly, it is possible to integrate a highly electronically conductive phase (such as silver) with a highly ionically conductive phase (such as yttria-stabilized bismuth oxide (YSB)) to achieve high ambipolar conductivities [5,6]. Dense membranes of these composites have been used for gas separation and electrosynthesis. The performance of these composite membranes depends critically on the ambipolar transport properties of the composites. For electrode applications, however, composites consisting of more than two phases are preferred to achieve high catalytic properties. One of the well-known examples is porous metal–ceramic composites used as electrodes in solid oxide fuel cells (SOFCs). The pores introduced can be considered as a third phase in the composites. The state-of-the-art anode for a SOFC based on yttria-stabilized zirconia (YSZ) is a porous composite consisting of Ni and YSZ. In this composite electrode, Ni is electronically

*Corresponding author. Email: meilin.liu@mse.gatech.edu

PII S0167-2738(96)00521-8

conductive, YSZ is ionically conductive [7–9], while pores are introduced to the composite to facilitate gas transport through the electrode and to accelerate electrode kinetics by increasing the number of active reaction sites, i.e., the triple-phase points or boundaries among Ni, YSZ, and gas phase. Another example is the composite electrodes used for all-solid-state lithium-ion rechargeable batteries. For a composite electrode based on $Li_xMn_2O_4$, for instance, a polyethylene oxide (PEO)-based electrolyte such as $p(EO)_8LiClO_4$ is typically used as the ionically conductive matrix phase, carbon black is used as the electronically conductive phase, while intercalation compound $Li_xMn_2O_4$ is dispersed uniformly throughout the composite [10].

The ambipolar conductivity is an important parameter which characterizes the simultaneous transport abilities of both ionic and electronic species in an MIEC and is given by [11]

$$\sigma_{amb} = \frac{\sigma_e \sigma_i}{\sigma_e + \sigma_i} + \frac{\sigma_i' - \sigma_i}{1 - \zeta}, \quad \zeta = \frac{\sigma_i' - \sigma_i}{\sigma_e} \tag{1}$$

where σ_e is the effective electronic conductivity, σ_i is the effective ionic conductivity, and σ_i' is the partial conductivity of ionic species under suppressed transport of electronic species (i.e., under the condition that the electronic current density, j_e, approaches zero),

$$\sigma_i' = -\left[\frac{\partial j}{\partial(\Delta V/\delta x)}\right]_{j_e=0,\ j\to 0} \tag{2}$$

where j is the current density and $\Delta V/\delta x$ is the potential gradient in the direction of current flow. When the external circuit is open, or the mixed conductor is under ambipolar diffusion condition, the current densities due to the motion of both ionic and electronic species are primarily determined by the ambipolar conductivity of the mixed conductor. Accordingly, one of the most fundamental questions about these composites is how their transport properties, particularly the ambipolar conductivity, are influenced by the volume fraction and geometrical distribution of each constituent phase.

Two basic approaches have been adopted to predict the conductivities of various composites. The traditional approach, such as the parallel model, the serial model, and the Maxwell model [12–14] has been successfully used to predict the conductivities of 'simple' composites. By simple we mean that either the phases in the composite are arranged regularly or the amounts of secondary phases are small so that only one phase is continuous. These traditional models, however, are incapable of predicting the observed sharp transitions in electrical properties of 'complex' composites. By complex we mean that the distribution of each constituent phase in the composite is irregular and the amounts of additional phases are significant. The second approach called percolation theory, which was originally developed to describe the phenomena of a fluid passing through a porous solid medium, was then adopted for prediction of electrical properties of two-phase composites with irregularly-distributed phases. The effective medium percolation theory (EMPT) is one of the most frequently used models when the effective conductivity of a composite is under consideration [15–21]. The percolation models developed for prediction of conductivities are applied only to two-phase composites. For a multi-phase composite, a generalized formula needs to be developed.

In this paper, the EMPT is first generalized to material systems composed of any number of randomly-distributed phases using a resistor network approach and a general equation for the effective conductivity of a multi-phase composite is obtained. The ambipolar transport properties of composite MIECs are then predicted as a function of volume fractions of their constituent phases using the generalized model. The predicted results for two-phase MIECs agree well with the experimental observations. The effect of distribution of each constituent phase on the electrical behavior of a multi-phase composite is still under investigation.

2. Effective conductivity of randomly-distributed multi-phase composites

2.1. Physical model of the systems

The electrical properties of a composite depend not only on the volume fraction of each constituent phase but also on the particular distribution of each

phase. To illustrate the significance of distribution, let's consider a metal–ceramic composite consisting of silver and YSB.

On one hand, consider a composite consisting of grains of silver and YSB, each grain being distributed arbitrarily. Previous experimental results indicate that a sharp transition in conductivity of the sample occurs when the volume fraction of silver approaches 34 vol% [22], as shown in Fig. 1(a). This means that the silver phase becomes continuous and the ambipolar conductivity of the composite reaches the maximum when the volume fraction of Ag is about 34%. The microstructure of a composite consists of 35 vol% silver and 65 vol% YSB is shown in Fig. 1(b) [23]. The composite was prepared by conventional ceramic processing. On the other hand, consider a YSB membrane containing a string of silver grains, each silver grain being in contact with the neighboring silver grains, as schematically shown in Fig. 2. In this case, there will be no sharp transition in conductivity of this sample since there is a continuous silver phase across the ceramic membrane. This means that, in principle, the ambipolar conductivity of this composite reaches the maximum as Ag content approaches zero.

Although the YSB membrane containing a silver string (or an array of silver string) may have high ambipolar conductivity, the usefulness of this arrangement is doubtful since an electrochemically functional mixed conductor should have good catalytic activities at the surface as well. For instance, when used for oxygen separation or as electrodes in SOFCs, the composite with randomly-distributed phases [Fig. 1(b)] is preferred to the composite containing a silver string (Fig. 2) simply because the former has much more active reaction sites (triple-phase points and boundaries) than the latter. In fact, the latter may even not be functional either used as a membrane for oxygen separation or as an electrode for an SOFC because of the lack of sufficient active reaction sites. Further, it is very difficult to control the specific distribution of phases in a composite since a lot of factors or processes can influence the distribution, such as wetting, surface tension, densification and coarsening during sintering, and other naturally-occurring processes during material processing. When none of these factors is dominant, random distribution can be a good approximation,

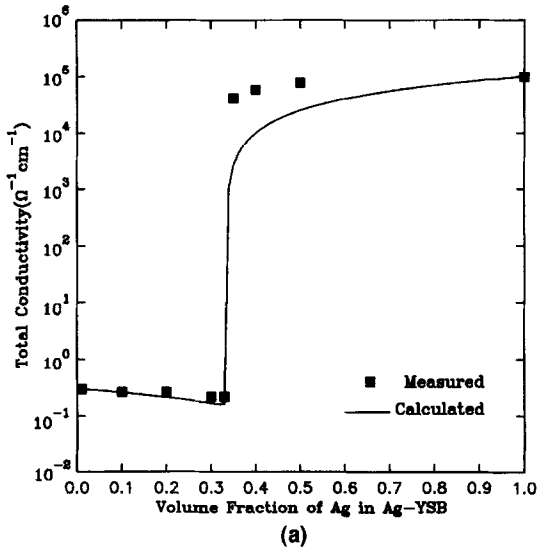

Fig. 1. (a) Measured and calculated total conductivities of Ag–YSB composites as a function of silver volume fraction and (b) an SEM micrograph for a 35 vol% Ag–65 vol% YSB composite prepared by conventional ceramic processing.

even though none of those factors is a completely random process.

In general, the exact distributions of the phases in

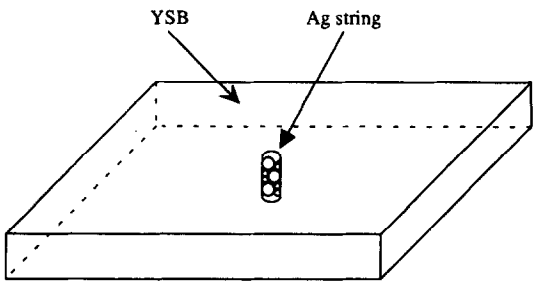

Fig. 2. A schematic showing a YSB electrolyte membrane containing a string of silver grains (or a silver wire).

a composite can be well characterized by distribution functions [24]. The effect of distribution on electrical properties of a composite will, however, not be discussed further in this paper. Instead, we will focus merely on composites in which the distribution of each phase is sufficiently random since random distribution is frequently observed in many composites which have practical significance.

A composite with randomly-distributed phases, or the physical model under consideration, is defined as follows. First, each constituent phase is composed of small particles (such as grains of different sizes and shapes). Second, the average size of the particles is much smaller than the dimension of the samples so that the number of particles counted in any direction in the composite is reasonably large. Third, the size of the particles is much greater than the mean free path of charge carriers so that the nature of conduction in each particle and in each phase is similar to that in the corresponding bulk phase with large dimension. Finally, the distribution of each phase in the composite is sufficiently random. By random distribution we mean that any specific particle has an equal probability of appearing in any position in the whole sample (in contrast, uniform distribution means that the same form or pattern of particle distribution is occurring throughout the sample). By sufficiently random we mean that the number fraction of particles in each phase counted in any direction can be adequately approximated by the volume fraction of the phase in the composite.

It is important to note that the particle size or shape can vary considerably. The particle size can have certain distribution as long as the largest particle size is reasonably smaller than the dimension of the sample, the smallest particle size is reasonably greater than the mean free path of charge carriers, and the particle sizes of all phases are comparable.

Depicted in Fig. 3 is an ideal microstructure generated by a computer for a two-phase composite [25], in which one phase is randomly distributed in the other phase. The distribution is completely random. In contrast, the microstructure of an Ag–YSB composite, prepared using conventional ceramic processing, is shown in Fig. 1(b). The distribution of silver in the Ag–YSB composite may not be completely random, but is sufficiently random, since the observed percolation transition in the conductivity of the composite can be predicted using the model for composites with randomly-distributed phases.

2.2. Resistor network approach

In this section, we will use an equivalent resistor network to approximate the steady-state electrical conduction of the complex composites described in the previous section. In fact, equivalent resistor networks have long been used in modeling simple composites [26–28]. The resistor network approach to be used for modeling a complex composite is, in essence, a generalization of the well-known parallel

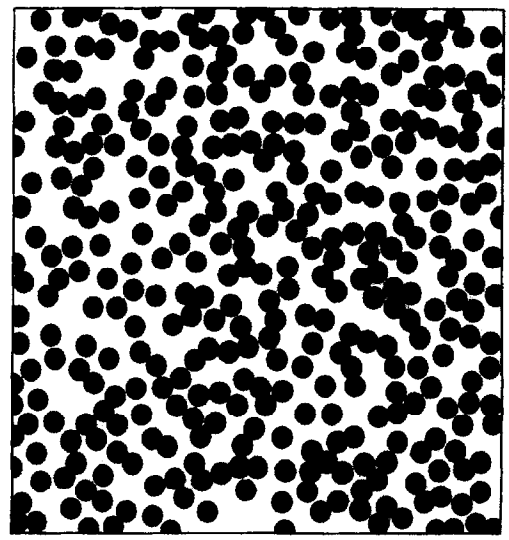

Fig. 3. Computer generated microstructure of a two-phase composite (volume fraction of the dark phase = 0.35). The dark phase is randomly distributed in the white phase.

and serial model for design of simple composite materials. The use of a resistor network to approximate a complex two-phase system in which one phase has zero conductivity was first proposed by Kirkpartrick [14,19]. Later, the approach was extended by other authors (such as Stephen [16]) to describe a complex system consisting of two non-zero-conductivity phases. In this paper we will further extend the resistor network approach to a multi-phase composite, a complex system consisting of any number of randomly-distributed phases. In addition, the physical picture of the resistor network will be made apparent through the construction of the resistor network. The value of coordination number (*Z*) in the resistor network and its physical meaning will also be clearly defined.

2.2.1. Construction of resistor network

An equivalent resistor network representing a composite can be obtained by dividing the composite into small cells, each having exactly the same shape and size. The dimension of each conducting cell is relatively small compared to the dimension of the particles so that the distribution of the constituent phases in the composite can be well approximated by the distribution of these cells. Note that the only possible shape of the cells will be parallelepiped in order to cover the whole space by repeating these cells. This is similar to the repeating of a unit cell in a crystal. Since each parallelepiped has 6 faces, each cell has a coordination number of 6, i.e., each cell is in direct contact with 6 neighboring cells. For simplicity yet without losing generality, let's assume the cells are cubic [Fig. 4(a)]. An arbitrary current flow in a cell can always be decomposed into three independent components along the three principle axes, such as X_1, X_2, and X_3 in Fig. 4. In each of the three principal directions, the electrical conduction within each cell can be approximated by a resistor [19]. Therefore, the conducting behavior of each cell can be equivalent to three resistors lying in the X_1, X_2, and X_3 axes and intersecting at the midpoint of each resistor (or six half-resistors), as shown in Fig. 4(b). If the cell under discussion is away from phase-boundaries, the three resistors will have the same resistance since the cell is cubic. This configuration is the same as the one shown in Fig. 4(c) in which six half-resistors are connected to one node.

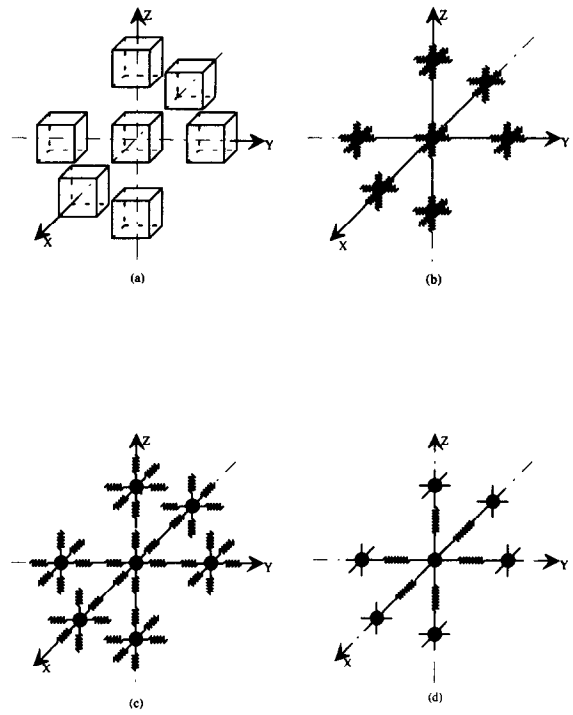

Fig. 4. Schematics showing the construction of a three-dimensional resistor network: (a) parallelepiped cells, (b) equivalent resistors in their principal directions, (c) rearrangement of the resistors, and (d) the equivalent resistor network.

Now combine every half-resistor with another half-resistor from its neighboring cell, the combined resistor will have the same resistance as a whole resistor [Fig. 4(d)]. It is clear that the number of resistors connected to each node is 6, or the coordination number Z of the resistor network is 6. In case a cell is across a phase-boundary or right next to a boundary, the resistors connected to the node at the body-center of the cell may have different resistances. However, each resistor should be primarily within one phase when the dimension of the cell is significantly smaller than the dimension of particles defined earlier. A cross-sectional view of the so-generated equivalent resistor network for a three-dimensional composite is shown in Fig. 5(a). Similarly, the equivalent resistor network will have a coordination number of 4 ($Z=4$) for a two-dimensional composite (such as a thin film) and a coordination number of 2 ($Z=2$) for a one dimensional composite (such as a composite wire).

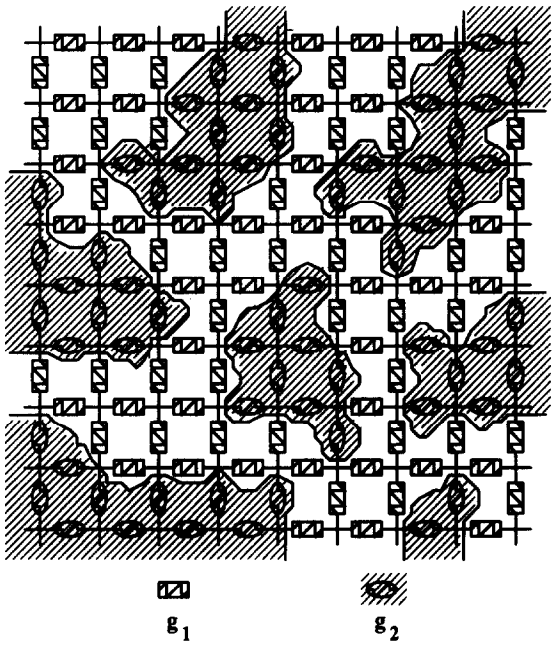

(a)

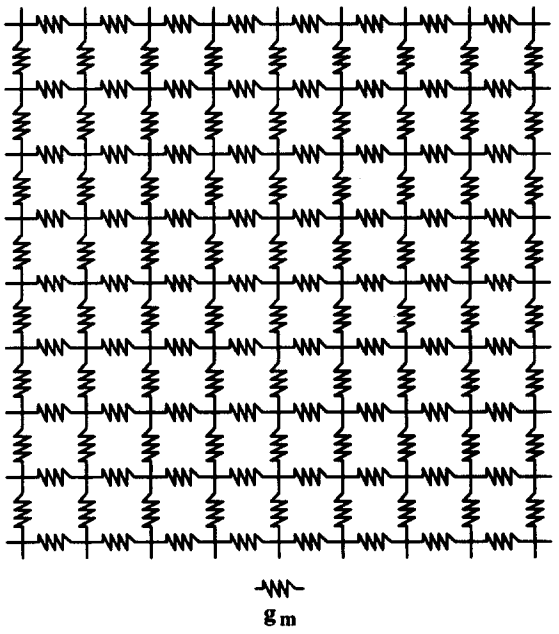

(b)

Fig. 5. Cross-sectional views of equivalent resistor networks for (a) a composite and (b) the corresponding effective medium.

The network so-constructed will be named as the 'composite network' in the following discussions. Now, imagine that the whole composite can be approximated by a homogenous medium with effective conductivity of the composite [29,30]. This homogeneous medium can also be approximated by a resistor network, in which all resistors are arranged geometrically the same way as in the composite network and all resistors have exactly the same conductance, as illustrated in Fig. 5(b). This resistor network is referred to as the 'effective network'.

2.2.2. Derivation of general formula for effective conductivity

Although our major concern is a three-dimensional composite, the following discussions are not limited to a three-dimensional composite situation. The conductance of a resistor in the composite network, g_k, can be related to its conductivity, σ_k, by a geometrical constant, c,

$$g_k = c\sigma_k. \tag{3}$$

Similarly, the conductance, g_m, and the conductivity, σ_m, of a resistor in the effective network are related as,

$$g_m = c\sigma_m. \tag{4}$$

When a voltage is applied to the effective network along a particular direction, the potential drop from one node to its nearest neighbor is a constant, V_m, such as the voltage between nodes A and B in Fig. 6(a). The effective network is equivalent to the circuit shown in Fig. 6(b) [14], in which the whole network except the resistor between A and B is considered as an equivalent circuit element H having conductance g'_{AB}. If the resistor between A and B is replaced by an arbitrary resistor with conductance g_k from the composite network, both the current passing through g_k and the voltage drop upon it will be changed. However, we can introduce a fictitious resistor with conductance g_f to be connected at points A and B, as shown in Fig. 6(c). When g_f takes on value of

$$g_f = g_m - g_k, \tag{5}$$

the total conductance of g_f and g_k remains g_m, and the effective network remains unchanged. In other words, the voltage dropped on the circuit element H

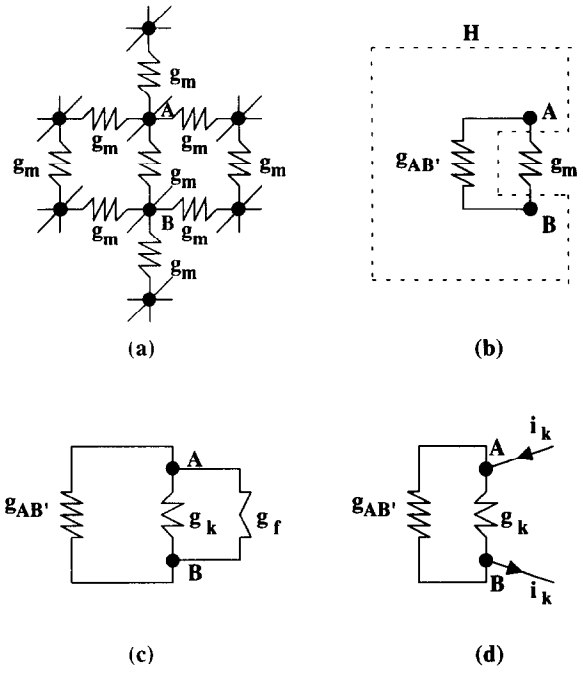

Fig. 6. Equivalent circuits used in calculating the effective conductivity of a composite (note that (a), (b), (c), and (d) are all equivalent).

and the current flowing through it will remain unchanged if the resistor g_m between A and B is replaced by g_k while a fictitious current of

$$i_k = V_m(g_m - g_k) \tag{6}$$

is introduced into the network at A and extracted out of the network at B, as shown in Fig. 6(d).

Now, let's re-examine the circuit shown in Fig. 6(d). Clearly, the introduced fictitious current i_k will cause a change in voltage drop upon resistor g_k, which is given by

$$V_k = \frac{i_k}{g_k + g'_{AB}} \tag{7}$$

where g'_{AB} is the conductance of the effective network as measured at nodes A and B when the resistor between them is removed. Note that g_k in Eq. (7) is the conductance of the corresponding resistor in the composite network.

This operation can be applied to every resistor in the effective network; each resistor in the effective network is replaced with the geometrically corresponding resistor in the composite network, together with a fictitious current or voltage. It is important to note that the network remains unchanged after each operation. When all these operations are done, the effective network is transformed to the composite network, in which each resistor is associated with a fictitious current (Eq. (6)) or a fictitious voltage change (Eq. (7)). When the number of resistors in an arbitrarily chosen direction, N, is sufficiently large and the distributions of all phases are sufficiently random as assumed earlier, the sum of all the voltage changes over each resistor in the arbitrarily chosen direction, defined by Eq. (7), should vanish [29], i.e.,

$$\sum_k V_k N p_k = 0 \tag{8}$$

where p_k is the volume fraction of component k with conductance g_k in the composite and Np_k is the number of resistors with conductance g_k in the direction. Clearly, all volume fractions of constituent phases should sum up to unity, i.e., $\Sigma_k p_k = 1$. Thus, Eq. (8) gives a criterion to determine the effective conductance of the network, g_m. Combining Eq. (6), Eqs. (7) and (8), we have

$$\sum_k \frac{NV_m(g_m - g_k)p_k}{g_k + g'_{AB}} = 0 \tag{9}$$

which is identical to

$$\sum_k \frac{(g_m - g_k)p_k}{g_k + g'_{AB}} = 0 \tag{10}$$

since N and V_m are constant. Also, it is clear that N, and hence the number of cells artificially created earlier, has no effects on the final results. Eq. (9) and Eq. (10) will prevail for any composites in which the distributions of constituent phases are sufficiently random.

The following resistor network analysis [14] indicates that the conductance of the effective network shown in Fig. 6(a) as measured at nodes A and B (g_{AB}) is equal to ($Z/2$) times the conductance of resistor g_m between A and B, i.e.,

$$g_{AB} = \frac{Z}{2} g_m \tag{11}$$

where Z is the coordination number. As seen from Fig. 7, Z resistors are connected to each node in the resistor network. Accordingly, a current introduced

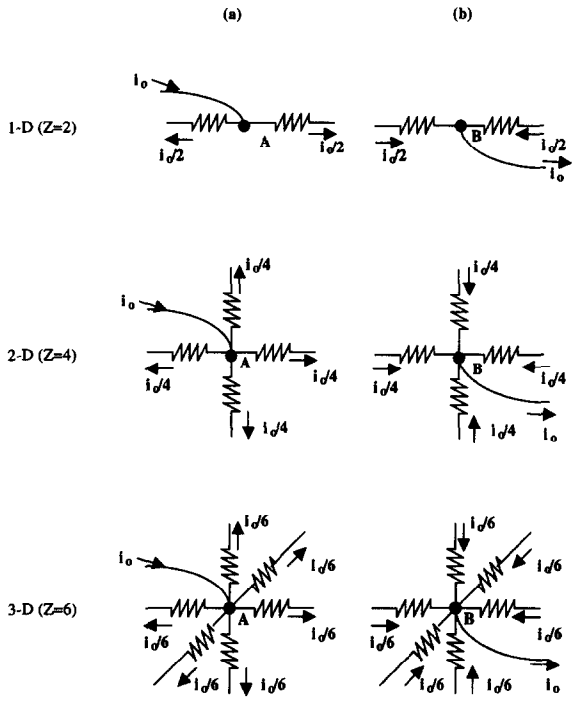

Fig. 7. (a) A fictitious current i_0 is injected at node A and collected at a very large distance away from A and (b) a fictitious current i_0 is introduced at a large distance away from node B and collected at B.

at or extracted from a node will flow to or from these Z resistors. The current flowing from node A to B through resistor g_m can be considered as the sum of the following two contributions: (i) a current introduced at A and extracted at a very large distance away from A in all directions, as shown in Fig. 7(a), and (ii) the same current introduced at infinity and extracted at B, as shown in Fig. 7(b). In each case, the current flowing through each of the Z resistors connected to the node is i_0/Z, where i_0 is the current introduced at A and extracted from B. Thus current passing through the resistor g_m between A and B is $2i_0/Z$, and the voltage drop across the resistor is $2i_0/(Zg_m)$. The conductance of the equivalent circuit as measured at A and B is then given by

$$g_{AB} = \frac{i_0}{2i_0/(Zg_m)} = \frac{Z}{2}g_m. \tag{12}$$

Therefore, g'_{AB} can be obtained as

$$g'_{AB} = g_{AB} - g_m = (\frac{1}{2}Z - 1)g_m. \tag{13}$$

Combining Eq. (13) with Eq. (10), we have

$$\sum_k \frac{g_m - g_k}{(Z/2-1)g_m + g_k} p_k = 0. \tag{14}$$

Substituting $g_m = c\sigma_m$ and $g_k = c\sigma_k$ into Eq. (14), we obtain

$$\sum_k \frac{\sigma_m - \sigma_k}{(Z/2-1)\sigma_m + \sigma_k} p_k = 0, \tag{15a}$$

$$\sum_k p_k = 1. \tag{15b}$$

Eqs. (15a) and (15b) is the general implicit expression for the steady-state effective conductivity of a composite consisting of any number of randomly-distributed constituent phases. Clearly, the effective conductivity depends merely on the coordination number (Z), the conductivity of each constituent phase (σ_k), and, the volume fraction of each phase (p_k) for this model.

It is important to emphasize, again, that the shape, the size, and the specific distribution of each component phase in the composite are not taken into consideration in this resistor network modeling. These factors may have significant effects on the effective conductivity of a composite and the percolation threshold. However, the derived equations are applicable as long as the distribution of each phase is sufficiently random and the dimension of the particles or phases is reasonable, that is, not too large to invalidate the randomness of distribution in any direction and not too small to less than the order of the mean free path of charge carriers. For most metal–ceramic composites prepared by conventional ceramic processing, the stated assumptions are reasonable and the derived equations are useful. The utility of Eqs. (15a) and (15b) will be demonstrated using a number of well-known composite MIECs in next section.

3. Ambipolar transport properties of MIECs

In order to predict the ambipolar transport properties of a composite, the effective electronic and ionic conductivities of a composite are considered separately. Thus, when the electronic resistivity of each constituent phase is used, we have a resistor

network to approximate the steady-state electronic conduction in the composite; similarly, when the ionic resistivity of each constituent phase is used, we have a resistor network to approximate the steady-state ionic conduction in the composite. When the motion of the ionic species is independent of the existence and transport of the electronic species and vice versa, the second term in the expression of the ambipolar conductivity (Eq. (1)) can be neglected, i.e.,

$$\sigma_{amb} \simeq \frac{\sigma_e \sigma_i}{\sigma_e + \sigma_i}. \tag{16}$$

If the interactions between the ionic and electronic species can not be neglected, Eq. (1) has to be used to predict the ambipolar conductivity. Strictly speaking, Eq. (16) was derived for homogeneous MIECs [11]. Under the assumption of this paper (as stated in Section 2.1), however, this equation is adequate for the purpose of this study since the composites under consideration are homogeneous on the macroscopic scale.

3.1. Two-phase composites

3.1.1. Formulation

For a composite consisting of two randomly-distributed phases, Eqs. (15a), (15b) become

$$\sum_{k=1}^{2} \frac{\sigma_m - \sigma_k}{(\frac{1}{2}Z-1)\sigma_m + \sigma_k} p_k = 0$$

$$= \frac{\sigma_m - \sigma_1}{\left(\frac{1}{2}Z-1\right)\sigma_m + \sigma_1} p_1 + \frac{\sigma_m - \sigma_2}{\left(\frac{1}{2}Z-1\right)\sigma_m + \sigma_2} p_2, \tag{17a}$$

$$p_1 + p_2 = 1. \tag{17b}$$

Solving for σ_m from Eqs. (17a) and (17b) for a three-dimensional composite, we find

$$\sigma_m = \frac{E_1 + \sqrt{E_1^2 + E_2}}{4} \tag{18}$$

where

$$E_1 = 3(p_1\sigma_1 + p_2\sigma_2) - (\sigma_1 + \sigma_2),$$

$$E_2 = 8\sigma_1\sigma_2.$$

Note that Eq. (18) is the same equation as obtained from the EMPT [21]. Thus, the derived general equation for a multi-phase composite, Eqs. (15a) and (15b), reduces to the equation for a two-phase composite as derived by the pioneers in the percolation theory [14,16,17,19,21].

Metal–ceramic composites are good examples of two-phase composites. A lot of metal–ceramic composites have been developed as mixed conductors for solid state ionic devices. Although the percolation theory has been verified for many two-phase composite systems [18,22], there is no information on ambipolar conducting behavior of composite MIECs, which involves the simultaneous transport of both ionic and electronic species. Modeling of the total and ambipolar conductivities of a two-phase composite MIEC will provide valuable guidance to the design and fabrication of composite mixed conductors. Let σ_1^e and σ_2^e be the electronic conductivities of phases 1 and 2, respectively, and σ_1^i and σ_2^i be the ionic conductivities of phases 1 and 2, respectively. The effective electronic conductivity of the composite is given by

$$\sigma_m^e = \frac{E_1^e + \sqrt{(E_1^e)^2 + E_2^e}}{4} \tag{19}$$

where

$$E_1^e = 3(p_1\sigma_1^e + p_2\sigma_2^e) - (\sigma_1^e + \sigma_2^e),$$

$$E_2^e = 8\sigma_1^e\sigma_2^e.$$

Similarly, the effective ionic conductivity of the composite is given by

$$\sigma_m^i = \frac{E_1^i + \sqrt{(E_1^i)^2 + E_2^i}}{4} \tag{20}$$

where

$$E_1^i = 3(p_1\sigma_1^i + p_2\sigma_2^i) - (\sigma_1^i + \sigma_2^i),$$

$$E_2^i = 8\sigma_1^i\sigma_2^i.$$

If the interaction between the ionic and the electronic charge carriers is negligible, the ambipolar conductivity of the composite conductor can be approximated as

$$\sigma^{i}_{amb} = \frac{\sigma^{e}_{m}\sigma^{i}_{m}}{\sigma^{e}_{m} + \sigma^{i}_{m}}. \quad (21)$$

This assumption is reasonable for a metal–ceramic composite such as Ag–YSB and Ni–YSZ, in which the electronic species are primarily confined in the metal phase and the ionic species are primarily confined in the ceramic phase. Further, the total conductivity of the composite is simply the sum of the ionic and the electronic conductivity, i.e.,

$$\sigma_{total} = \sigma^{e}_{m} + \sigma^{i}_{m}. \quad (22)$$

3.1.2. Calculation and implication

Composites of Ag and $Bi_{1.5}Y_{0.5}O_3$ have been developed for gas separation and electrocatalysis while composites of Ni and YSZ have been extensively used as anode materials for YSZ based solid oxide fuel cells. LSCF itself is a good cathode material for SOFCs; however, Ag–LSCF composites exhibit better mechanical flexibility and higher catalytic properties [31]. Using Eqs. (19)–(21), we can predict the effective electronic, ionic, total, and ambipolar conductivities of the composite as a function of the volume fraction of the metal phase (phase 2) in the composite. The approximate conductivities of each phase used in the calculation are listed in Table 1 [32–34]. The curves of σ^{e}_{m}, σ^{i}_{m}, σ_{total}, and σ_{amb} as a function of volume fraction of the metal phase are shown in Fig. 8, Fig. 9, Fig. 10 and Fig. 11, respectively. One immediate observation is that the three composite systems fall into two categories; Ag–YSB and Ni–YSZ composites have very similar behavior whereas the properties of Ag–LSCF composites are quite different. This is because the electronic conductivity of LSCF is much greater than that of YSB or YSZ. The implication of these calculations can be described as follows.

First, sharp transitions in effective conductivities are observed in the Ag–YSB and Ni–YSZ composites. The percolation threshold occurs at $p_2 = 1/3$ for the effective electronic, total, and ambipolar conductivities and at $p_2 = 2/3$ for the effective ionic and ambipolar conductivities. This means that the metal

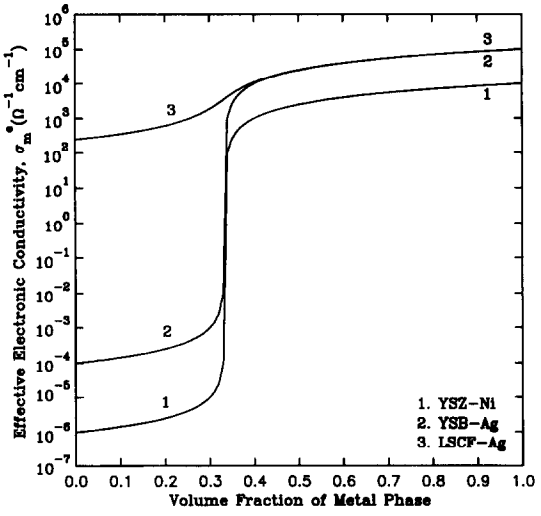

Fig. 8. Effective electronic conductivities of dense metal–ceramic composites, as calculated using Eq. (19).

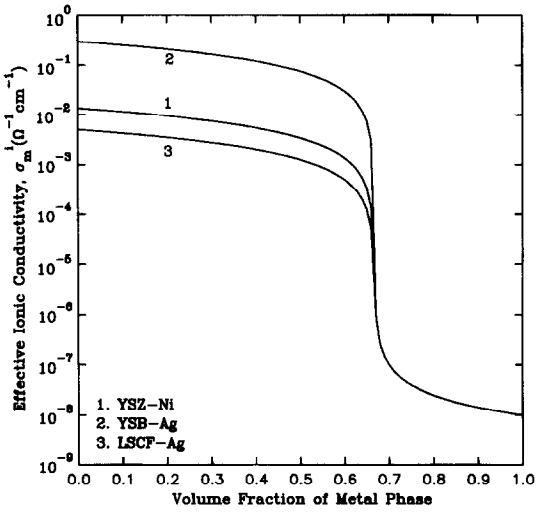

Fig. 9. Effective ionic conductivities of dense metal–ceramic composites, as calculated using Eq. (20).

Table 1
Conductivities of materials at 750°C

Material	Ag	Ni	YSB	YSZ	LSCF [34]
σ_e (Ω^{-1} cm^{-1})	10^5 [29]	10^4 [29]	10^{-4}	10^{-6}	2.5×10^2
σ_i (Ω^{-1} cm^{-1})	10^{-8}	10^{-8}	0.3 [21]	0.014 [30]	5×10^{-3}

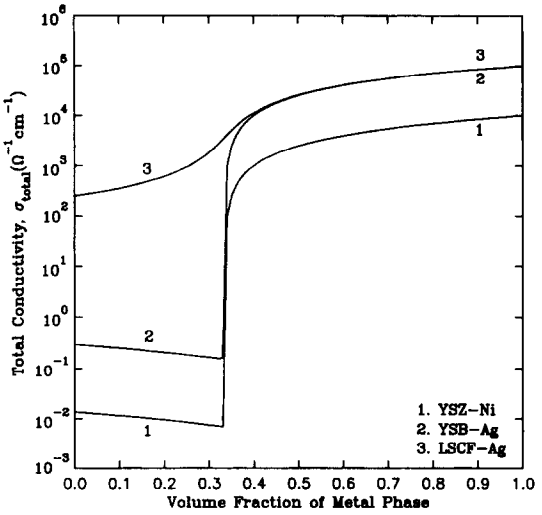

Fig. 10. Total conductivities of dense metal–ceramic composites, as calculated using Eq. (22).

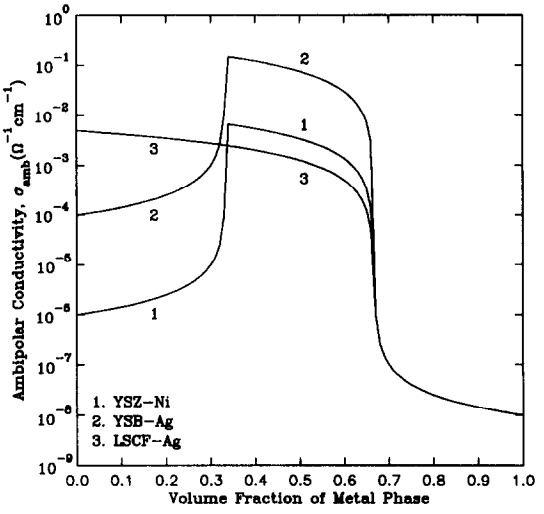

Fig. 11. Ambipolar conductivities of dense metal–ceramic composites, as calculated using Eq. (21).

phase becomes continuous when its volume fraction is greater than 1/3 and the ceramic phase becomes discontinuous when the volume fraction of metal phase is greater than 2/3. The predicted sharp transition in total conductivity of Ag–YSB composite actually has been verified by experiment [22], as shown in Fig. 1(a). Similar phenomena have been observed by many other authors, such as, Chen et al. [6], Gaucker [35], and Mazanec et al. [36]. Mathematically, the percolation threshold for a two-phase composite should be

$$p_2^c = \left(\frac{2}{Z}\right)\frac{\left(\frac{1}{2}Z-1\right)\sigma_1 - \sigma_2}{\sigma_1 - \sigma_2}, \tag{23}$$

as derived in Appendix A. Thus, when $\sigma_1 \ll \sigma_2$, $p_2^c = 2/Z = 1/3$ for a three-dimensional system.

Second, the two sharp percolation transitions of the ionic and electronic conductivities lead to a composition range from 1/3 to 2/3, in which the ambipolar conductivity is much higher than those in other regions (Fig. 11). This suggests that in order to achieve high ambipolar conductivity, the volume fraction of each phase must be within 1/3~2/3. A composition with volume fraction of metal phase slightly greater than 1/3 should have the highest ambipolar conductivity, because the electronic conductivity of the metal phase is in orders of magnitude greater than the ionic conductivity of the ceramic phase.

Third, for LSCF–Ag composites, the effective electronic and total conductivities increase gradually with silver content while the ionic and ambipolar conductivities decrease continuously with the volume fraction of Ag. The percolation transitions in the total and electronic conductivities are gradual and occur at $p_1 = 1/3$ while the transitions in ionic and ambipolar conductivities are sharp and occur at $p_2 = 2/3$. This suggests that large differences in conductivities is necessary in order to have a sharp percolation transition. Also, it is clear that the addition of Ag to LSCF will not improve the ambipolar conductivity because the electronic conductivity of LSCF is much greater than the ionic conductivity of LSCF.

Finally, further calculations on other material systems indicate that when there are large differences between the ionic conductivities of the two phases or between the electronic conductivities of the two phase, sharp transition in conductivities are expected at 1/3 volume fraction of the more conductive phases. Further, when the effective electronic conductivity is much larger than the effective ionic conductivity, the optimum volume fraction of the more conductive phase (p_2^*) at which the ambipolar conductivity is maximized, always tends to be slightly greater than 1/3 (Fig. 12). These predicted trends,

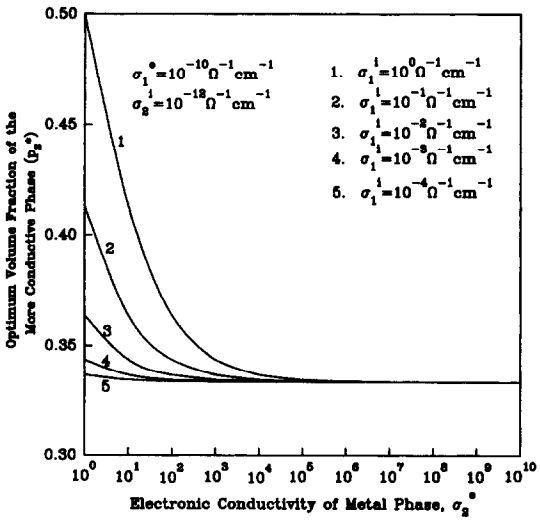

Fig. 12. Optimum volume fraction of the more conductive phase for maximum ambipolar conductivity of a composite as a function of σ_1^i and σ_2^e, while σ_1^e and σ_2^i are kept constant ($\sigma_1^e = 10^{-10}$ Ω^{-1} cm^{-1} and $\sigma_2^i = 10^{-12}$ Ω^{-1} cm^{-1}).

which are particularly true for many metal–ceramic composites used as MIECs, have provided valuable guidance in design of composite membranes for oxygen separation [5,23].

3.2. Three-phase composites

For a three-dimensional ($Z=6$) composite MIEC consisting of three randomly-distributed phases, Eqs. (15a) and (15b) become

$$\frac{\sigma_m - \sigma_1}{2\sigma_m + \sigma_1}p_1 + \frac{\sigma_m - \sigma_2}{2\sigma_m + \sigma_2}p_2 + \frac{\sigma_m - \sigma_3}{2\sigma_m + \sigma_3}p_3 = 0, \tag{24a}$$

$$p_1 + p_2 + p_3 = 1. \tag{24b}$$

Eq. (24a) can be expanded as

$$\begin{aligned} 4\sigma_m^3 &+ [2p_1\sigma_2 + 2p_1\sigma_3 + 2p_2\sigma_1 + 2p_2\sigma_3 \\ &+ 2p_3\sigma_1 + 2p_3\sigma_2 - 4p_1\sigma_1 - 4p_2\sigma_2 - 4p_3\sigma_3]\sigma_m^2 \\ &- [2p_1\sigma_1\sigma_2 + 2p_1\sigma_1\sigma_3 + 2p_2\sigma_1\sigma_2 + 2p_2\sigma_2\sigma_3 \\ &+ 2p_3\sigma_1\sigma_3 + 2_{p_3}\sigma_2\sigma_3 - p_1\sigma_2\sigma_3 \\ &- p_2\sigma_1\sigma_3 - p_3\sigma_1\sigma_2]\sigma_m - \sigma_1\sigma_2\sigma_3 = 0. \end{aligned} \tag{25}$$

Once we know the conductivities of the component phases and their volume fractions, the effective conductivity of the composite can be calculated from the above equation. This will be illustrated by applying the equation to two technologically important composite mixed conductors: porous metal–ceramic electrodes for SOFCs and dense three-phase composite electrodes based on $Li_xMn_2O_4$ for lithium-ion batteries.

3.2.1. Porous metal–ceramic mixed conductors

Dense membranes of Ag–YSB composite MIEC have been used for oxygen separation. For electrode applications, however, a certain amount of pore volume is preferred in order to facilitate gas transport through the electrode and to maximize the number of active reaction sites. For a porous Ag–YSB cathode used in SOFCs [37], the reduction of oxygen occurs at the reaction sites (i.e., the triple phase points or boundaries among Ag, YSB, and gaseous O_2) according to

$$\tfrac{1}{2}O_2 + 2e' \rightarrow O^{2-}.$$

The kinetics of this reaction is influenced by several factors, including (1) the number of reaction sites and the intrinsic catalytic activity of the reaction sites for interfacial reactions such as adsorption of O_2, dissociation of O_2 into atoms, and charge transfer; (2) the transport of O^{2-} away from reaction sites through the solid phase; (3) the transport of electrons (e′) to the reaction site through the solid phase; and (4) the transport of gaseous O_2 to the reaction site through the pores. The transport of e′ and O^{2-} in the solid phase is determined by the ambipolar conductivity of the electrode.

On one hand, it is desired to increase the porosity in order to increase the number of reaction sites and to facilitate the gas transport through the pores. On the other hand, the composite electrode must have adequate ambipolar conductivity to deliver the e′ to and O^{2-} away from the reaction sites. The objective of the following analysis is to predict the effect of porosity and volume fraction of silver on the ambipolar transport properties of the solid phase of the electrode, not to optimize the overall performance of the electrode.

The introduction of a third phase, pores, will alter

the total effective conductivity and the ambipolar conductivity of the porous composites. The actual role of pores in a porous electrode can be rather complicated. If there is rapid transport of ionic and electronic species along the pore surfaces due to surface diffusion, then an additional phase should be assigned to represent the surface or interfacial layer in the composite. Measured electronic and ionic conductivities of the surface layer can be used to model the behavior of the composite. For simplicity, the conductivities of the pores are assumed to be zero. Under this assumption, the conductivity of a porous solid with porosity less than 15% can be roughly estimated using Bruggeman equation [28],

$$\sigma_m = \sigma_0(1-p)^{3/2} \tag{26}$$

where σ_0 is the conductivity of the pore-free solid and p is the porosity. More generally, Baumgarter et al. gave a similar equation [38],

$$\sigma_m = \sigma_0(1-p)^x \tag{27}$$

where x ranges from 1.5 to 3. With Eq. (25), however, we can precisely predict the conducting behavior of a porous metal–ceramic composite with any porosity, if the distribution of all three phases is sufficiently random.

Formulation

Substituting $\sigma_3 = 0$ into Eq. (25), we have

$$4\sigma_m^2 + [2p_1\sigma_2 + 2p_2\sigma_1 + 2p_3\sigma_1 + 2p_3\sigma_2 - 4p_1\sigma_1 - 4p_2\sigma_2]\sigma_m - [2p_1\sigma_1\sigma_2 + 2p_2\sigma_1\sigma_2 - p_3\sigma_1\sigma_2] = 0. \tag{28}$$

Since $p_1 + p_2 + p_3 = 1$, this can be rewritten as

$$2\sigma_m^2 + [3(p_1\sigma_1 + p_2\sigma_2) - (\sigma_1 + \sigma_2)]\sigma_m + \left[(p_1 + p_2) - \frac{1}{2}p_3\right]\sigma_1\sigma_2 = 0. \tag{29}$$

The reasonable root of this equation is

$$\sigma_m = \frac{F_1 + \sqrt{F_1^2 + F_2}}{4} \tag{30}$$

where

$$F_1 = 3(p_1\sigma_1 + p_2\sigma_2) - (\sigma_1 + \sigma_2),$$

$$F_2 = 4\sigma_1\sigma_2[3(p_1 + p_2) - 1].$$

In order to ensure that σ_m is positive, the volume fraction of the solid phase must be greater than 1/3 ($p_1 + p_2 \geq 1/3$) or the porosity must be less than 2/3 ($p_3 < 2/3$). When the porosity is greater than 2/3 ($p_3 \geq 2/3$), Eq. (29) is no longer valid and we have to go back to the original Eq. (25) in order to obtain an appropriate general solution, and then let σ_3 approach zero. Since it is unusual for a practical composite electrode to have porosity greater than 2/3, $p_3 < 2/3$ is assumed so that Eq. (30) is appropriate in the following discussion.

In order to simplify our discussion, let

$$x_1 = p_1/(1-p) \tag{31}$$

and

$$x_2 = p_2/(1-p) \tag{32}$$

where p is the porosity of the composite, i.e., $p = p_3$. It can be seen that x_1 and x_2 are the relative volume fractions of phases 1 and 2 in a pore-free, two-phase metal–ceramic composite, respectively. Obviously, $x_1 + x_2 = 1$.

Then, p_1 and p_2 can be obtained from two parameters, x_2 and p,

$$p_1 = (1-p)(1-x_2), \tag{33}$$

$$p_2 = (1-p)x_2. \tag{34}$$

The effective electronic conductivity of the porous metal–ceramic composite is then given by

$$\sigma_m^e = \frac{F_1^e + \sqrt{(F_1^e)^2 + F_2^e}}{4} \tag{35}$$

where

$$F1^e = 3(1-p)[(1-x_2)\sigma_1^e + x_2\sigma_2^e] - (\sigma_1^e + \sigma_2^e),$$

$$F_2^e = 4\sigma_1^e\sigma_2^e[3(1-p) - 1],$$

Similarly, the effective ionic conductivity is

$$\sigma_m^i = \frac{F_1^i + \sqrt{(F_1^i)^2 + F_2^i}}{4} \tag{36}$$

where

$$F_1^i = 3(1-p)[(1-x_2)\sigma_1^i + x_2\sigma_2^i] - (\sigma_1^i + \sigma_2^i),$$

$$F_2^i = 4\sigma_1^i\sigma_2^i[3(1-p) - 1],$$

The ambipolar conductivity and the total conductivity of the composite can be calculated using Eq. (21) and Eq. (22), respectively.

Calculations and implications

The conducting behavior of porous Ag–$Bi_{1.5}Y_{0.5}O_3$ composites are predicted as a function of the porosity and the relative volume fraction of each phase using Eq. (35), Eq. (36), Eq. (21), and Eq. (22). A number of observations can be made from these calculations.

Fig. 13 indicates that the effective electronic conductivities decrease while the percolation threshold values increase with porosity. This means that the volume fraction of metal phase (x_2) needed to form a continuous metal phase increases with porosity, varying from 1/3 for a dense composite (zero porosity) to about 2/3 for a composite with 50% porosity. This is because the pores interrupt the continuity of the metal phase.

As can be seen from Fig. 14, the effective ionic conductivity and percolation threshold value of metal content (x_2) decrease with porosity. Obviously, the pores interrupt the continuity of ceramic phase as well. This means that the volume fraction of YSB needed to form a continuous ceramic phase also increases with porosity. The threshold values of percolation transition for effective electronic and ionic conductivities are summarized in Fig. 17.

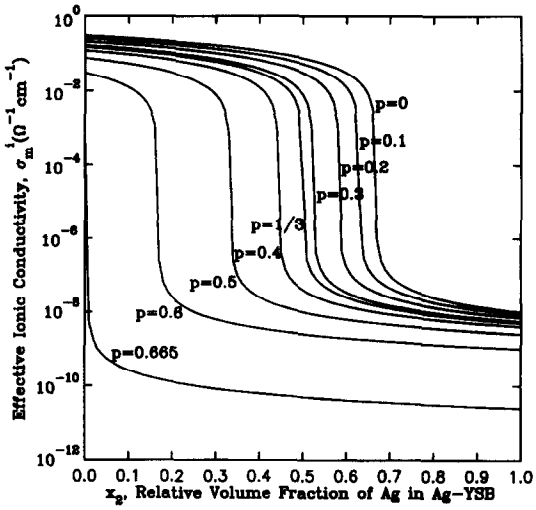

Fig. 14. Effective ionic conductivities of porous Ag–$Bi_{1.5}Y_{0.5}O_3$ composites, as calculated using Eq. (36).

Further, as shown in Fig. 15, the total conductivity of the composite also decreases with porosity since both ionic and electronic conductivities decrease with porosity. The range of metal content (x_2) within which the composite has a relatively high total conductivity shrinks with porosity, varying from

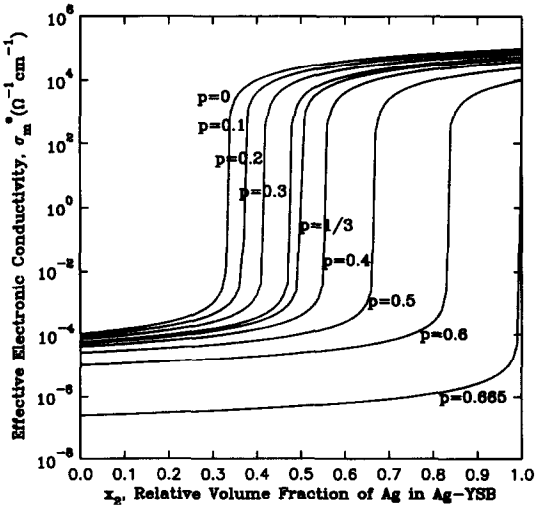

Fig. 13. Effective electronic conductivities of porous Ag–$Bi_{1.5}Y_{0.5}O_3$ composites, as calculated using Eq. (35).

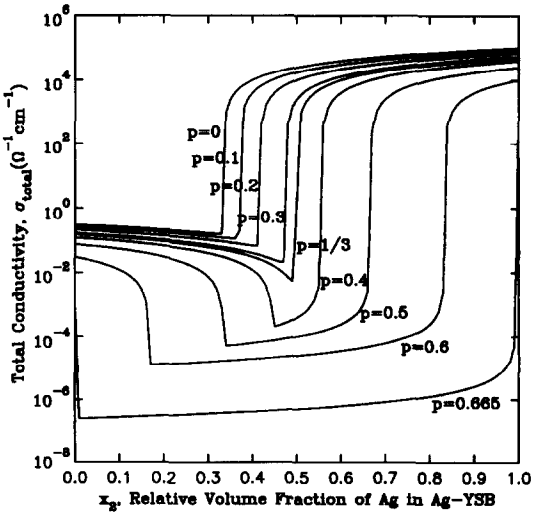

Fig. 15. Total conductivities of porous Ag–$Bi_{1.5}Y_{0.5}O_3$ composites.

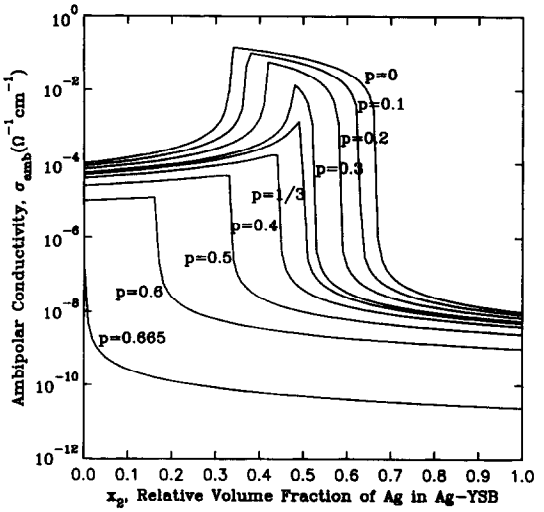

Fig. 16. Ambipolar conductivities of porous Ag–$Bi_{1.5}Y_{0.5}O_3$ composites.

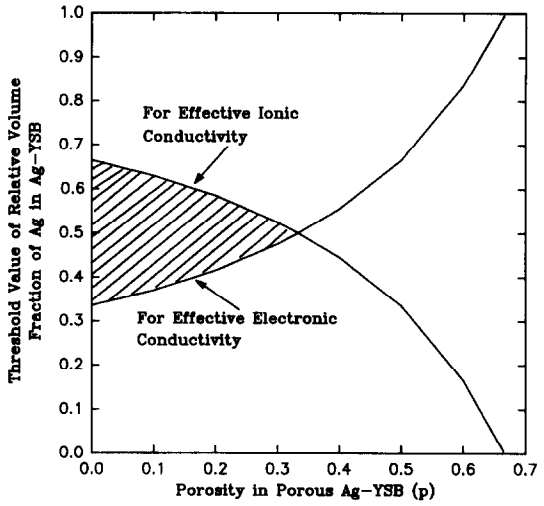

Fig. 17. Effect of porosity on threshold values of the relative volume fraction of silver phase in porous Ag–YSB composites.

1/3~1 for a dense composite to 2/3~1 for a composite with 50% porosity.

Fig. 16 shows that a range of metal content still exists in which the ambipolar conductivity is much higher than that in other regions. However, the width of this range decreases with porosity, varying from 1/3~2/3 for a dense composite to a single point (at 50%) for a composite with porosity of 1/3. For example, the optimum volume fraction of silver (x_2), at which the ambipolar conductivity is maximized, should be about 50% for an electrode with 30% porosity. Thus, it is necessary to ensure the composition fall within the shaded region in Fig. 17 in order to have relatively high ambipolar conductivity. These predictions have been used as valuable guidance in design of porous metal–ceramic composite electrodes for SOFCs and other solid state ionic devices [31,37,40].

Finally, in order to optimize the transport of both ionic and electronic species in the composite, the porosity should be within 30% since the ambipolar conductivity decreases dramatically with porosity when porosity is greater than 30%, as shown in Fig. 18. This is because it is impossible to keep both ceramic and metal phases continuous when the porosity is greater than 1/3. Although the ambipolar conductivity increases with the decrease in porosity, certain amount of porosity is desired in order to

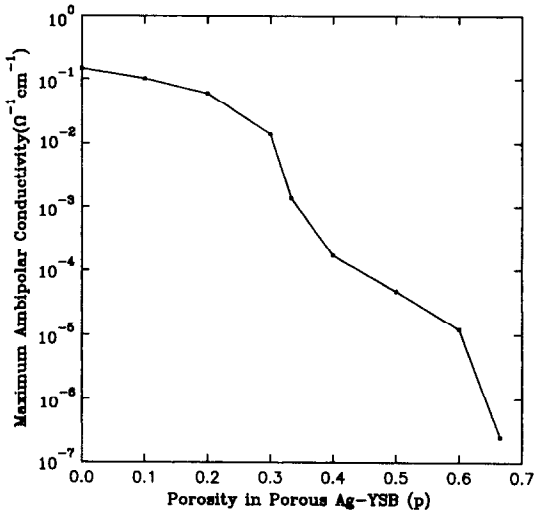

Fig. 18. Effect of porosity on maximum ambipolar conductivities of porous Ag–YSB composites.

enhance gas transport and the catalytic activity of a composite electrode as discussed earlier. Optimization of porosity in a metal–ceramic composite electrode, which involves simultaneous consideration of ambipolar transport in the solid phase, gas transport through the pores, and the number and nature of the triple-phase points and boundaries, will be discussed in a subsequent communication [41].

3.2.2. Composite electrodes based on $Li_xMn_2O_4$

A composite electrode based on $Li_xMn_2O_4$ for all-solid-state lithium-ion batteries usually contain three phases: carbon black powder, $Li_xMn_2O_4$ powder, and a polymer-based electrolyte. The polymer electrolyte such as $p(EO)_8LiClO_4$ typically functions as the matrix phase of the composite. The powders of carbon and $Li_xMn_2O_4$ can be considered to be randomly-dispersed in the polymer electrolyte. Typically, the electronic and the ionic conductivities of carbon and polymer electrolyte used are known and fixed while the electronic and ionic conductivities of $Li_xMn_2O_4$ vary quite significantly during charging or discharging. In general, the volume fraction of $Li_xMn_2O_4$ should be maximized while the volume fractions of carbon and polymer electrolyte should be minimized to achieve high energy density. Yet, composite electrode with insufficient amount of carbon black or polymer electrolyte will have inadequate ambipolar conductivity and hence poor rate capability. Accordingly, the fundamental question to be addressed in this modeling is how to optimize the ambipolar conductivity of the composites by tailoring the volume fraction of each constituent phase.

To find the effective conductivity of the composite, we have to solve Eqs. (24a) and (24b). Because of the complexity of the equation, a straight-forward, analytical expression for effective conductivity is not available and Eqs. (24a) and (24b) have to be solved numerically. Let's consider carbon powder as phase 1, $Li_xMn_2O_4$ powder as phase 2, and $p(EO)_8LiClO_4$ polymer electrolyte as phase 3. The conductivities of these materials are taken as follows: $\sigma_1^e = 10^3$ $\Omega^{-1}\,cm^{-1}$ and $\sigma_1^i = 10^{-10}$ $\Omega^{-1}\,cm^{-1}$ for carbon (phase 1), and $\sigma_3^e = 10^{-10}$ $\Omega^{-1}\,cm^{-1}$ and $\sigma_3^i = 10^{-4}$ $\Omega^{-1}\,cm^{-1}$ for PEO-based electrolyte (phase 3). The conductivity of $Li_xMn_2O_4$ (phase 2) is reported to be in the order of 10^{-6} $\Omega^{-1}\,cm^{-1}$ [39], depending on the degree of insertion. In order to simplify the calculation, the volume fraction of $Li_xMn_2O_4$ (phase 2) was set at 50%.

Figs. 19 and 20 show the dependence of the total and ambipolar conductivities of the composites on the electronic conductivity of $Li_xMn_2O_4(\sigma_2^e)$ while its ionic conductivity is kept at a constant, $\sigma_2^i = 10^{-6}$ $\Omega^{-1}\,cm^{-1}$. The implication of these calculations can be described as follows.

First, when the volume fraction of carbon (p_1) is

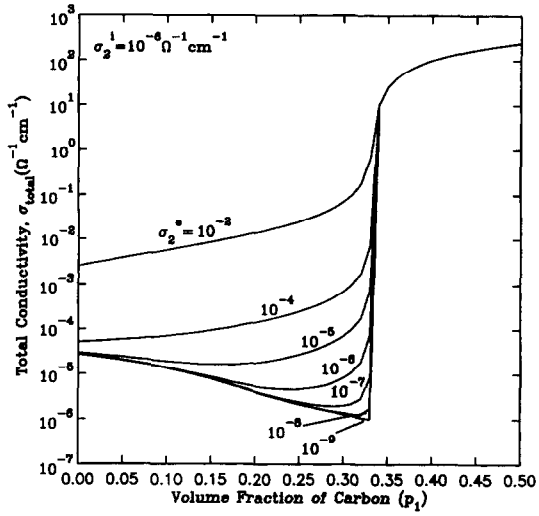

Fig. 19. Total conductivities as a function of carbon content (p_1) at different electronic conductivities of $Li_xMn_2O_4$ (phase 2) while the ionic conductivity of $Li_xMn_2O_4$ is kept at 10^{-6} $\Omega^{-1}\,cm^{-1}$ ($p_1 + p_3 = 50\%$ and $p_2 = 50\%$).

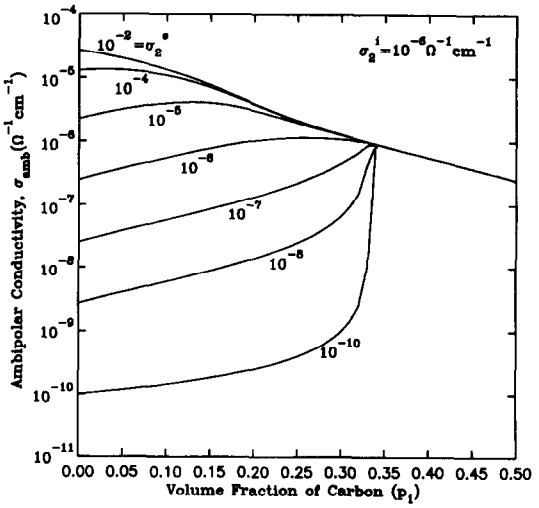

Fig. 20. Ambipolar conductivities as a function of carbon content (p_1) at different electronic conductivities of $Li_xMn_2O_4$ while the ionic conductivity of $Li_xMn_2O_4$ is kept at 10^{-6} $\Omega^{-1}\,cm^{-1}$ ($p_1 + p_3 = 50\%$ and $p_2 = 50\%$).

greater than 1/3, both ambipolar and total conductivities of the composite are independent of the electronic conductivity of $Li_xMn_2O_4$. This is because the continuous carbon phase provides adequate electronic conductivity so that the electronic transport through the $Li_xMn_2O_4$ phase has no significant

effect. Accordingly, the ambipolar conductivity of the composite is primarily controlled by the effective ionic conductivity.

Second, when the carbon phase is not continuous ($p_1 < 1/3$), both total and ambipolar conductivities depend strongly on the electronic conductivity of $Li_xMn_2O_4$ (σ_2^e). When the electronic conductivity of $Li_xMn_2O_4$ is relatively low ($\sigma_2^e < 10^{-3}\ \Omega^{-1}\ cm^{-1}$), increasing the amount of carbon (phase 1) improves the ambipolar conductivity. Accordingly, the volume fraction at which the maximum ambipolar conductivity is obtained (p_1^*) increases with the decrease of σ_2^e. When the electronic conductivity of $Li_xMn_2O_4$ is sufficiently high ($\sigma_2^e > 10^{-3}\ \Omega^{-1}\ cm^{-1}$), on the other hand, adding carbon (phase 1) only lowers the ambipolar conductivity since the $Li_xMn_2O_4$ phase provides adequate electronic conductivity and the ambipolar conductivity is primarily determined by the effective ionic conductivity. However, the total conductivity always increases with addition of carbon (phase 1) because the electronic conductivity of carbon is much greater than the conductivities of any other phases in the composite.

Third, percolation transition occurs at $p_1 = 1/3$ for the total conductivity and the sharpness of this transition depends strongly on the electronic conductivity of the $Li_xMn_2O_4$ phase. For the ambipolar conductivity, however, a percolation transition can be observed at $p_1 = 1/3$ only when $\sigma_2^e < 10^{-7}\ \Omega^{-1}\ cm^{-1}$.

Figs. 21 and 22 show the dependence of the total and ambipolar conductivities of the composite on the ionic conductivities of $Li_xMn_2O_4$ while its electronic conductivity is kept at a constant, $\sigma_2^e = 10^{-5}\ \Omega^{-1}\ cm^{-1}$.

As shown in Fig. 21, a sharp transition in total conductivity occurs at $p_1 = 1/3$ and the percolation threshold is independent of the ionic conductivity of $Li_xMn_2O_4$. When the carbon phase is discontinuous, the total conductivity of the electrode increases with the ionic conductivity of $Li_xMn_2O_4$ (σ_2^i).

Fig. 22 indicates that when p_1 is less than 10%, the ambipolar conductivity is insensitive to the ionic conductivity of $Li_xMn_2O_4$ (σ_2^i). This is because the polymer electrolyte (phase 3) is continuous and the ionic conductivity of the composite is mainly controlled by the polymer electrolyte. On the other hand, when the volume fraction of carbon (p_1) is greater than 1/6, the polymer electrolyte phase becomes discontinuous (since $p_1 + p_2 > 2/3$ and hence $p_3 < 1/3$). Accordingly, the ambipolar conductivity of the composite depends critically on the ionic conductivity of $Li_xMn_2O_4$ (σ_2^i): (i) when $\sigma_2^i > 10^{-4}\ \Omega^{-1}\ cm^{-1}$, percolation in ambipolar conductivity

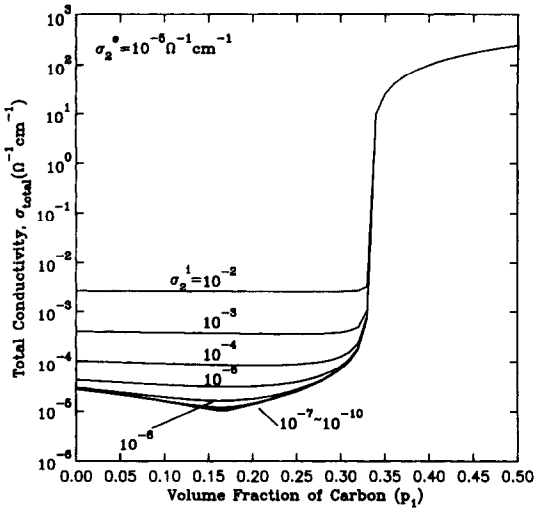

Fig. 21. Total conductivities as a function of carbon content (p_1) at different ionic conductivities of $Li_xMn_2O_4$ while the electronic conductivity of $Li_xMn_2O_4$ is kept at $10^{-5}\ \Omega^{-1}\ cm^{-1}$ ($p_1 + p_3 =$ 50% and $p_2 = 50\%$).

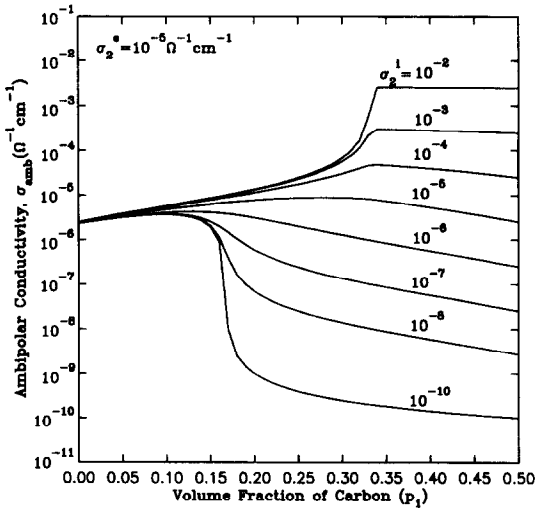

Fig. 22. Ambipolar conductivities as a function of carbon content (p_1) at different ionic conductivities of $Li_xMn_2O_4$ while the electronic conductivity of $Li_xMn_2O_4$ is kept at $10^{-5}\ \Omega^{-1}\ cm^{-1}$ ($p_1 + p_3 = 50\%$ and $p_2 = 50\%$).

occurs at $p_1 = 1/3$; (ii) when $\sigma_2^i < 10^{-7}\ \Omega^{-1}\ cm^{-1}$, percolation in ambipolar conductivity occurs at $p_1 = 1/6$; and (iii) when $10^{-7}\ \Omega^{-1}\ cm^{-1} < \sigma_2^i < 10^{-4}\ \Omega^{-1}\ cm^{-1}$, or when $\sigma_2^i \approx \sigma_2^e$, the volume fraction of carbon (phase 1) has little effect on the ambipolar conductivity.

4. Summary

Resistor network analysis has led to a general equation for predicting the ionic, electronic, and ambipolar transport behavior of a composite MIEC consisting of any number of randomly-distributed phases. For a three-dimensional, two-phase composite MIEC, the percolation threshold is found at 1/3 volume fraction of the more conductive phase. The ambipolar conductivity is relatively high when the volume fraction of each phase is within the range of 1/3 to 2/3. This is because within this range both phases are continuous. This has been used as a guidance in developing dense membranes of metal–ceramic composite mixed conductors. For a multiphase composite, the percolation threshold varies. For a porous metal–ceramic composite, the percolation threshold increases with porosity since pores interrupt the continuity of solid phases. Accordingly, the range of volume fractions over which high ambipolar conductivities are expected narrows with porosity. Therefore, the porosity and the relative volume fractions of the two solid phases should be carefully controlled in order to maintain the continuity of both solid phases and hence to achieve high ambipolar conductivities. For a three-phase composite electrode based on $Li_xMn_2O_4$, the ambipolar conductivity depends strongly on the volume fraction of the three phases and the conductivities of the $Li_xMn_2O_4$ phase in the composite. High ambipolar conductivity can be achieved by increasing the conductivities of $Li_xMn_2O_4$ and by tailoring the volume fractions of the three phases.

5. List of symbols

c	geometric factor, cm
g_{AB}	conductance of the effective network as measured at nodes A and B, Ω^{-1}
g'_{AB}	conductance of the effective network without the resistor between A and B, as measured at nodes A and B, Ω^{-1}
g_f	conductance of a fictitious resistor, Ω^{-1}
g_k	conductance of resistor k in the composite network, Ω^{-1}
g_m	conductance of a resistor in the effective network, Ω^{-1}
j	current density, A/cm^2
j_e	electronic current density or current density due to the motion of electronic species, A/cm^2
i_0	current introduced at node A and extracted at node B in Fig. 7, A
i_k	fictitious current, A
N	number of resistors in an arbitrary direction in each network, dimensionless
p	porosity of a metal–ceramic composite, dimensionless
p_k	volume fraction of phase k, dimensionless
p_2^c	critical volume fraction of phase 2 at the percolation point
s	$(Z/2) - 1$
V_k	change in voltage drop upon resistor g_k due to current i_k, V
V_m	potential drop from one node to its nearest neighbor, V
$\Delta V/\delta x$	potential gradient in the direction of current flow, V/cm
x_k	relative volume fraction of phase k in a pore-free, two-phase composite, dimensionless
y	$\ln \sigma_m$
Z	coordination number
σ_{amb}	ambipolar conductivity of a composite, $\Omega^{-1}\ cm^{-1}$
σ_e	effective electronic conductivity, $\Omega^{-1}\ cm^{-1}$
σ_k	conductivity of phase k, $\Omega^{-1}\ cm^{-1}$
σ'_i	partial conductivity of ionic species under suppressed transport of electronic species, $\Omega^{-1}\ cm^{-1}$
σ_m	effective conductivity of a composite, $\Omega^{-1}\ cm^{-1}$
σ_m^e	effective electronic conductivity of a composite, $\Omega^{-1}\ cm^{-1}$
σ_m^i	effective ionic conductivity of a composite, $\Omega^{-1}\ cm^{-1}$
σ_{total}	total conductivity of a composite, $\Omega^{-1}\ cm^{-1}$
ζ	$(\sigma'_i - \sigma_e)/\sigma_e$, dimensionless

6. Abbreviations

MIEC	mixed ionic–electronic conductor
YSB	yttria-stabilized bismuth oxide
YSZ	yttria-stabilized zirconia
SOFC	solid oxide fuel cell
PEO	polyethylene oxide
EMPT	effective medium percolation theory
LSCF	$La_{1-x}Sr_xCo_{1-y}Fe_yO_3$

Acknowledgments

This work was supported by National Science Foundation under award No. DMR-9357520 and Electric Power Research Institute under contract No. RP1676-19.

Appendix A

In general, the percolation threshold for a two-phase composite can be determined as follows: Let $y=\ln \sigma_m$ and $s=(Z/2)-1$, then $\sigma_m=e^y$, $Z=2(1+s)$. Eqs. (17a), (17b) can be rewritten as

$$se^{2y}+(\sigma_2 p_1+\sigma_1 p_2-s\sigma_1 p_1-s\sigma_2 p_2)e^y-\sigma_1\sigma_2=0. \tag{A-1}$$

Differentiating both sides of Eq. (A-1) with respect to p_2 and recognizing $\partial p_1/\partial p_2=-1$ and $e^y\neq 0$, we have

$$2se^y\frac{\partial y}{\partial p_2}+(1+s)(\sigma_1+\sigma_2)e^y+(\sigma_2 p_1+\sigma_1 p_2-s\sigma_1 p_1-s\sigma_2 p_2)\frac{\partial y}{\partial p_2}=0. \tag{A-2}$$

Differentiating both sides of Eq. (A-2) with respect to p_2, we have

$$2se^y\left(\frac{\partial y}{\partial p_2}\right)^2+2se^y\frac{\partial^2 y}{\partial p_2^2}+(1+s)(\sigma_1-\sigma_2)\frac{\partial y}{\partial p_2}+(\sigma_2 p_1+\sigma_1 p_2-s\sigma_1 p_1-s\sigma_2 p_2)\frac{\partial^2 y}{\partial p_2^2}=0. \tag{A-3}$$

Note that at a percolation point, $|\partial y/\partial p_2|$ reaches the maximum, i.e., $\partial y/\partial p_2\neq 0$ and $\partial^2 y/\partial p_2^2=0$. Accordingly, Eq. (A-3) can be reduced to,

$$2se^y\frac{\partial y}{\partial p_2}=-(1+s)(\sigma_1-\sigma_2). \tag{A-4}$$

Inserting Eq. (A-4) into Eq. (A-2) yields

$$\left(\frac{1+s}{2s}\right)(\sigma_1-\sigma_2)(\sigma_2 p_1+\sigma_1 p_2-s\sigma_1 p_1-s\sigma_2 p_2)e^{-y}=0. \tag{A-5}$$

Since $\sigma_1\neq\sigma_2$ (otherwise there will be no percolation phenomena), p_1 and p_2 must satisfy

$$\sigma_2 p_1+\sigma_1 p_2-s\sigma_1 p_1-s\sigma_2 p_2=0 \tag{A-6}$$

at the percolation point.

Note that $p_1+p_2=1$, then the critical point for the percolation is

$$p_2^c=\frac{1}{1+s}\frac{s\sigma_1-\sigma_2}{\sigma_1-\sigma_2}=\left(\frac{2}{Z}\right)\frac{\left(\frac{1}{2}Z-1\right)\sigma_1-\sigma_2}{\sigma_1-\sigma_2}. \tag{A-7}$$

It can be verified that $\partial y/\partial p_2\neq 0$ at $p_2=p_2^c$. Clearly, when $\sigma_1\ll\sigma_2$, Eq. (A-7) becomes

$$p_2^c=\frac{1}{1+s}=\frac{2}{Z}=\begin{cases}1/3, & Z=6\ \text{(3-D)},\\ 1/2, & Z=4\ \text{(2-D)},\\ 1, & Z=2\ \text{(1-D)},\end{cases} \tag{A-8}$$

and when $\sigma_1>>\sigma_2$, Eq. (A-7) becomes

$$p_2^c=1-\frac{2}{Z}=\begin{cases}2/3, & Z=6\ \text{(3-D)},\\ 1/2, & Z=4\ \text{(2-D)},\\ 0, & Z=2\ \text{(1-D)}.\end{cases} \tag{A-9}$$

The effective conductivity of the composite at the critical point is given by

$$\sigma_m=\sqrt{\frac{\sigma_1\sigma_2}{2}}. \tag{A-10}$$

References

[1] T. Inoue, T. Setoguchi, K. Eguchi and H. Arai, Solid State Ionics 35 (1989) 285.
[2] A.W. Smith, F.W. Meszaros and C.D. Amata, J. Am. Ceram. Soc. 49 (1966) 240.

[3] R.J.H. Voorhoeve, J.P. Remeika, L.E. Trimble, A.S. Cooper, F.J. Disalvo and P.K. Gallagher, J. Solid State Chem. 14 (1975) 395.
[4] R.B. Golder, T.E. Hass, G. Seward, K.K. Wong, P. Norton, G. Foley, G. Berera, G. Wei, S. Schulz and R. Chapman, Solid State Ionics 28 (1988) 1715.
[5] M. Liu, A. Joshi, Y. Shen and A. Krist, US patent No. 5,273,628 (1993); US patent No. 5,478,444 (1995);
[6] C.S. Chen, B.A. Boukamp, H.J.M. Bouwmeester, G.Z. Cao and H. Kruidhof, Solid State Ionics 76 (1995) 23.
[7] T. Kawada, H. Yokokawa, M. Doyika, M. Mori and, T. Iwata, J. Electrochem. Soc. 137 (1990) 3042.
[8] D.C. Fee and J.P. Ackerman, Abstracts of the 1983 Fuel Cell Seminar (Orlando, FL, November 13–16, 1983) pp. 11–14.
[9] A.O. Isenberg, Abstracts of the 1982 Fuel Cell Seminar (Newport Beach, CA, November 14–18, 1982) pp. 154–156.
[10] C.A. Angell, C. Liu and E. Sanchez, Nature 362 (1993) 137.
[11] M. Liu, in: Proc. 1st Int. Symp. on Ionic and Mixed Conducting Ceramics, eds. T.A. Ramanarayanan and H.L. Tuller, PV 91–12 (The Electrochemical Society, Pennington, NJ, 1991) pp. 191.
[12] R.L. Mccullough, Comp. Sci. Tech. 22 (1985) 3.
[13] J.M. Wimmer, H.C. Graham and N.M. Tallen, Microstructural and polyphase effects, in: Electrical Conductivity in Ceramics and Glass, ed. N.M. Tallan (Dekker, New York, 1974) p. 619.
[14] S. Kirkpatrick, Rev. Modern Phys. 45 (1973) 574.
[15] D.S. Mclachlan, Michael Blaszkiewicz and R.E. Newnham, J. Am. Ceram. Soc. 73 (1990) 2187.
[16] D.A. Stephen, Lectures in disordered systems, in: Critical Phenomena (Lecture Notes in Physics), ed. F.J.W. Hahner (Springer-Verlag, 1983).
[17] S.R. Broadbent and J.M. Hammersley, Proc. Camb. Soc. 53 (1957) 629.
[18] M.F. Bell, M. Sayer, D.S. Smith and P.S. Nicholson, Solid State Ionics 9 and 10 (1983) 731.
[19] S. Kirkpatrick, Phys. Rev. 27 (1971) 1722.
[20] S.W. Martin, Solid State Ionics 51 (1992) 19.
[21] D.G. Ast, Phys. Rev. Lett. 33 (1974) 1042.
[22] Y. Shen, M. Liu, D. Taylor, S.A. Bolagopal, A.Joshi and K. Krist, in: Proc. 2nd Int. Symp. Ionic and Mixed Conducting Ceramics, eds. T.A. Ramanarayanan, W.L. Worell, H.L. Tuller (The Electrochemical Society, Pennington, NJ, 1994) p. 574.
[23] H. Hu and M. Liu, Development of Thin-Film, Mixed-Conductive Membranes for Oxygen Separation (GRI annual report, 1995).
[24] P. Louis and A.M. Gokhale, Acta Mater. 44 (1996) 1519.
[25] S. Yang and A.M. Gokhale, private communication.
[26] J.C. Maxwell, Electricity and Magnetism, Vol. 1, 3rd ed. (Clarendon Press, Oxford 1892) p. 440.
[27] H. Fricke, J. Phys. Chem. 57 (1953) 934.
[28] M.P. Anderson and S. Ling, J. Electronic Mater. 19 (1990) 1161.
[29] D.A.G. Bruggeman, Ann. Phys. 24 (1935) 636.
[30] R. Landauer, J. Appl. Phys. 23 (1952) 779.
[31] H. Hu and M. Liu, in: The Role of Ceramics in Electrochemical Devices, eds. P.N. Kumta et al., Ceramic Transactions, Vol. 65 (American Ceramic Society, Westerville, OH, 1995) p. 355.
[32] E.A. Brandes, Smithells Metals Reference Book, 6th ed. (Butterworth, London, 1983).
[33] T.H. Etsell and S.N. Flengas, Chem. Rev. 70 (1970) 339.
[34] L.-W. Tai, M.M. Nasrallah and H.U. Anderson, in Proceedings of the 3rd International Symposium on Solid Oxide Fuel Cells, eds. S.C. Singhal and H. Iwahara, PV93-4, The Electrochemical Society, Pennington, NJ (1993).
[35] L.J. Gauckler, Solid State Ionics 75 (1995) 203.
[36] T.J. Mazanec et al., Solid State Ionics 53–56 (1992) 111.
[37] Z. Wu and M. Liu, in Proceeding Volume of the 188th meeting of the Electrochemical Society, October 1995, Chicago, IL, in press.
[38] C.E. Baumgartner, R.H. Arendt, C.D. Iacovangelo and B.R. Karas, J. Electrochem. Soc. 131 (1984) 2217.
[39] G. Pistoia, D. Zane and Y. Zhang, J. Electrochem. Soc 142 (1995) 2551.
[40] H. Hu and M. Liu, J. Electrochem. Soc. 143 (1996) 859.
[41] Z. Wu and M. Liu, J. Electrochem. Soc., to be submitted.